A new voltage control scheme for active medium-voltage (MV) networks

Georgios C. Kryonidis, Charis S. Demoulias, Grigoris K. Papagiannis *

Abstract

The main objective of this paper is the effective voltage regulation in radial medium-voltage (MV) distribution networks with high distributed generation (DG) penetration, ensuring near-minimum active power losses. For this purpose, a new control strategy with low computational complexity is proposed. The method exploits the reactive power capability of DG units to mitigate overvoltages in coordination with the on-load tap changer of the high-/medium-voltage transformer to achieve power losses reduction. This is attained by introducing a time delay allocation method based on the graph theory to prioritise the response of DG units. The control scheme is further enhanced by the active participation of MV loads in the voltage regulation process, contributing to the reactive power control of DG units. To evaluate the performance of the proposed control strategy, time-domain and time-series simulations are performed in an extended radial MV network. The former demonstrates the robustness and fast response of the proposed control scheme, while the latter highlights its improved power system performance over existing centralised as well as decentralised control methods.

Keywords: Distributed power generation, loss minimization, on-load tap changer (OLTC), reactive power control, voltage control.

1. Introduction

Sustainable energy is considered as one of the most challenging targets, set by local administrations and international organisations, to reduce the carbon footprint and the fossil fuel dependence [1]. This is achieved by providing incentives – in terms of feed-in tariffs or quota obligations – to install distributed generation (DG) units, mainly consisting of renewable energy sources [2]. Nevertheless, the rapid deployment of DG units over the last

*School of Electrical and Computer Engineering, Aristotle University of Thessaloniki, P.O. Box 486, Thessaloniki GR-54124, Greece, e-mail: grigoris@eng.auth.gr

decade has invoked voltage rise issues in the distribution grid, limiting the further penetration of DG [3].

Traditionally, medium-voltage (MV) networks have been designed by the distribution system operators (DSOs) on the assumption of passive grid operation. As a result, the voltage regulation process was mainly performed by the on-load tap changer (OLTC) of the high-/medium-voltage (HV/MV) transformer and by the feeder capacitors or series voltage regulators [4]. However, these techniques fail to mitigate overvoltages in active networks with high DG penetration. The main reason lies in the fact that overvoltage is a local problem of the network [5], whereas the OLTC control concurrently manages all network nodes. Furthermore, the activation of feeder capacitors has an adverse effect on the mitigation of overvoltages. Another alternative involves reinforcing the grid, which, however, is an expensive solution for DSOs.

The voltage rise problem can be effectively addressed by incorporating reactive power control (RPC) techniques into DG units [6–24], acting as a local countermeasure to this issue. In the literature, the RPC methods can be classified into decentralised, distributed, centralised, and hybrid approaches.

The distinctive feature of the decentralised control schemes is that control actions are individually performed by each DG unit, based only on local measurements. The authors in [6] employ the reactive power capability of DG units to fully compensate the voltage rise caused by the active power injections. Nevertheless, unnecessarily high reactive power consumption may be observed. A decentralised method is proposed in [7] to tackle a two-objective problem, i.e. the overvoltage mitigation and the loss minimisation. Although this method is valid, conflicts between these objectives may appear in cases of high DG penetration. This problem has been partially addressed in [8], but the applicability of the developed method is limited to active feeders where only DG units are connected. In [9], an on-line optimisation-based voltage regulation method has been developed, which, however, may introduce inaccuracies in the presence of multiple DG units. The integration of the $Q(P)$ and $Q(V)$ droop control characteristics into the DG units has been thoroughly investigated in [10], while an offline coordination procedure has been proposed in [11] and [12], respectively. Moreover, artificial intelligence techniques are applied in [13] to define the

2

voltage thresholds for the activation of the RPC in each DG unit. Nevertheless, all of these methods are characterised by the uncoordinated real-time operation of DG units, leading to increased network losses.

To address the issues posed by the decentralised control, a distributed control strategy is proposed in [14]. According to this approach, the operational settings of each DG unit are determined based on local measurements and on the information acquired by the neighboring units. Additionally, a hybrid approach of the RPC is proposed in [15], combining both the decentralised and distributed control schemes. However, the main drawbacks of these methods include slow convergence rates and possible local minimum solutions.

In the centralized control scheme, a central controller monitors the network and determines the set-points for all DG units at each time instant. This controller is usually located at the DSO level. The relevant research works can be classified into two main categories based on whether they use optimisation techniques or not. Considering the first category, the introduction of optimisation techniques in the distribution grids forms a mixed-integer nonlinear optimisation problem characterised by increased computational complexity and local minimum solutions [16]. On the other hand, in the second category, the proposed solutions lack of optimisation procedures, focusing only on the secure and reliable network operation within permissible limits. More specifically, the authors in [17] and [18] use an analytical and approximate calculation of the sensitivity matrix to dispatch the reactive power among the DG units. In [19], OLTC and DG units are combined in a cooperative framework to address only voltage rise issues. Additionally, a centralised solution with no optimisation techniques is presented in [20], where an updated version of the distribution management system (DMS) is proposed, taking into account the reactive power capability of DG units. The off-line coordination of the OLTC and the network capacitors is proposed in [21], neglecting the participation of the DG units in the voltage regulation process.

In [22], a hybrid centralised-decentralised control strategy is proposed, in which the central controller is activated to optimise the network operation in case the decentralised voltage regulation control fails. An enhancement of [7] is proposed in [23], employing a central controller to decide the most appropriate objective at each time instant. In [24], the droop characteristics of all DG units are recalculated in a regular basis by solving an

3

optimisation problem. However, these hybrid methods present the same disadvantages as those observed in the centralised control schemes.

In this paper, a hybrid centralised-decentralised voltage regulation strategy for radial MV networks is proposed, aiming at the minimisation of network losses by properly co-ordinating the response of the DG units, the MV loads, and the OLTC of the HV/MV transformer. Its distinct features include: 1) near optimal solutions compared to the de-centralised approaches, 2) fast convergence against the distributed control schemes, and 3) low computational complexity compared to the centralised control strategies. The proposed method uses a time delay allocation procedure based on the graph theory to distribute the reactive power among the DG units, while the inherent inductive behaviour of the loads is exploited for the first time as a supplementary means for the overvoltage mitigation. Fur-thermore, the OLTC control acts in coordination with DG units and MV loads to further reduce network losses.

2. Theoretical framework

The voltage regulation in conjunction with the minimisation of network losses constitutes an optimisation problem. To solve this problem, three different types of network elements are involved, namely the DG units, the MV loads, and the OLTC of the HV/MV transformer. The DG units provide reactive power locally, since this is considered an effective voltage regulation method in MV distribution networks due to the relatively low R/X ratio of the lines [6]. On the other hand, MV loads generally consist of commercial and industrial loads, as well as low-voltage (LV) networks, connected to the MV level via MV/LV transformers. These loads are equipped with reactive power compensation devices, e.g. capacitor banks, to compensate their inherent inductive behaviour. Therefore, they can be exploited, similarly to the DG units, as controllable reactive power sources by switching on/off capacitor banks.

The combined operation of these network elements forms a mixed-integer nonlinear op-timisation problem, where the objective function is the minimisation of network losses as follows:

$$\min \sum_{i \in N} P_{\text{loss},i} \tag{1}$$

4

where N denotes the set of branches and of network nodes omitting the slack bus, while $P_{\text{loss},i}$ is the active power loss of the i-th branch.

The equality constraints of the optimisation problem include the power flow equations and the OLTC operation. Assuming the HV/MV transformer is modelled as a series impedance referred to the MV side, the power flow equations can be expressed mathematically by:

$$V_i^2 = \{V_{pr(i)}^2 + 2(A_i R_i + B_i X_i)$$
$$+ [V_{pr(i)}^4 + 4(A_i R_i + B_i X_i)V_{pr(i)}^2 - 4(A_i X_i - B_i R_i)^2]^{1/2}\}/2 \quad \forall i \in N \quad (2)$$

$$P_{\text{loss},i} = R_i(A_i^2 + B_i^2)/V_i^2 \quad \forall i \in N \tag{3}$$

$$Q_{\text{loss},i} = X_i(A_i^2 + B_i^2)/V_i^2 \quad \forall i \in N \tag{4}$$

Eq. (2) is used for the calculation of the network voltages, while (3) and (4) calculate the active ($P_{\text{loss},i}$) and reactive ($Q_{\text{loss},i}$) power losses of the i-th branch, respectively. V_i and $V_{pr(i)}$ denote the voltage magnitudes of the i-th node and of the previous adjacent node, respectively, whereas R_i and X_i are the resistance and the reactance of the i-th branch. A_i and B_i are the active and reactive power flowing through the i-th branch and are calculated according to

$$A_i = \sum_{j \in N_{\text{d},i}} P_j - \sum_{j \in N_{\text{d},n(i)}} P_{\text{loss},j} \tag{5}$$

$$B_i = \sum_{j \in N_{\text{d},i}} Q_j - \sum_{j \in N_{\text{d},n(i)}} Q_{\text{loss},j}. \tag{6}$$

$N_{\text{d},i}$ is the set of nodes located downstream of the i-th node, while P_j and Q_j denote the active and reactive power injections of the j-th node, respectively. $n(i)$ are the nodes located right after the i-th node. Furthermore, the OLTC operation is modelled by discretely varying the voltage magnitude (V_0) of the slack bus as follows:

$$V_0 = V_{\text{hv}}/\{m[1 + tap(\delta/100)]\} \tag{7}$$

where V_{hv} is the voltage magnitude of the HV grid, m is the voltage transformation ratio, tap stands for the tap position of the OLTC, and δ is the percentage variation of the transformation ratio per tap position change.

To maintain the network voltages within permissible limits and to avoid congestion issues, the following inequality constraints are introduced:

$$V_{\text{min}} \leq V_i \leq V_{\text{max}} \quad \forall i \in N \tag{8}$$

$$I_i \leq I_{\text{max},i} \quad \forall i \in N \tag{9}$$

Here, V_{min} and V_{max} are the minimum and the maximum permissible voltage limits determined by the DSO, while I_i and $I_{\text{max},i}$ are the current magnitude and the thermal limit of the i-th branch, respectively. Additionally, (10)-(11) represent the boundary limits of the control variables:

$$Q_{\text{min},i} \leq Q_i \leq Q_{\text{max},i} \quad \forall i \in N_{\text{dg}} \cup N_{\text{load}} \tag{10}$$

$$tap \in D \tag{11}$$

where N_{dg} and N_{load} are the set of network nodes in which the DG units and the loads are connected. Q_i is the reactive power produced by either the DG unit or the load connected to the i-th node, whereas $Q_{\text{min},i}$ and $Q_{\text{max},i}$ are the corresponding permissible limits. The reactive power of loads is treated as a continuous variable in the optimisation problem. This can be justified by the fact that, in industrial loads, capacitors are switched on/off at a resolution of 6-12 kVAr which is very small compared to the reactive power exchanged in the MV feeder. Finally, D is the discrete set of the available tap positions.

The optimisation problem of (1)-(11) presents an increased computational complexity which is mainly caused by three factors. The first corresponds to the inherent network non-linearities. The second is the use of a discrete control variable to model the OLTC operation, and finally the third one is the extensive size of MV networks. Consequently, conventional optimisation approaches are rather ineffective, since they suffer from local minimum solu-

tions. On the contrary, heuristic or metaheuristic techniques can overcome this burden, but they are considerably time-consuming and thus cannot be applied in real field conditions.

3. Proposed voltage regulation strategy

Scope of the proposed method is to solve the optimisation problem following a rule-based approach. For this purpose, a generic and straightforward procedure is introduced to coordinate the operation of the network elements participating in the voltage regulation process. In this way, the computational complexity is reduced and near-optimal solutions can be achieved. An analytical description of the developed control strategy is carried out in the next subsections, where the proposed operation for each network element type is presented including also their coordinated operation.

3.1. Reactive power control of DG units

Initially, a mathematical analysis is performed to investigate the impact of the DG selection on the network losses, regarding the voltage regulation of a specific node. More specifically, according to the *LinDistFlow* equations of [7], for a given voltage regulation at node v (ΔV_v), the necessary reactive power change of the DG unit connected to node q (ΔQ_q) is approximately calculated by:

$$\Delta Q_q \simeq \frac{V}{\sum\limits_{i \in Path_q \cap Path_v} X_i} \Delta V_v \qquad (12)$$

where V is the nominal voltage of the network and $Path_q$ denotes the set of nodes belonging to the path from the slack bus to node q. The corresponding network losses are estimated according to

$$\sum_{i \in N} P_{\text{loss},i} \simeq \frac{1}{V^2} [\sum_{i \in N} R_i \tilde{A}_i^2 + \sum_{i \in Path_q} R_i (\tilde{B}_i + \Delta Q_q)^2 + \sum_{i \in N \setminus Path_q} R_i \tilde{B}_i^2]. \qquad (13)$$

where $\tilde{A}_i$ and $\tilde{B}_i$ are calculated using (5) and (6), respectively, neglecting the terms related to losses, since they constitute a small portion of the actual power flowing through the i-th branch [7].

7

Depending on the relative position of node q with respect to node v, the following three cases are considered:

1) $Path_q = Path_v$. This is the reference case, in which the DG unit is connected to the regulated node v.

2) $Path_q \supset Path_v$, i.e. the DG unit is located downstream of the node v. In such a case, the same amount of reactive power as in the reference case is needed, which is verified by (12). Nevertheless, the network losses of (13) are increased, since a more distant node is used compared to the reference case.

3) $(Path_q \cap Path_v) \subset Path_v$. The DG unit is connected to the upstream nodes, resulting in an increased amount of reactive power compared to the reference case. Furthermore, it can be proved that network losses are also increased, assuming a constant R/X ratio along the feeder, which is the normal case for a typical MV feeder.

Consequently, the main outcome of the above analysis can be summarized in the following statement: Assuming the voltage regulation of a specific node, the network losses are minimized if the reactive power control is allocated only to the DG unit connected to this node.

The proposed reactive power allocation method is based on the above important outcome to tackle overvoltages in radial MV networks, minimizing the power losses at the same time. More specifically, for a given loading condition of the network, the node with the maximum voltage is the target node for the voltage regulation process.Furthermore, according to [25], the maximum network voltage is more likely to appear at the nodes where DG units are connected. As a result, the DG unit connected to the target node will absorb reactive power to mitigate overvoltage with minimum losses. Nevertheless, as the DG unit absorbs reactive power, the voltage profile along the network changes and a different network node may present the maximum voltage. In such a case, this node becomes the target node and the corresponding DG unit starts absorbing reactive power. This procedure continues till overvoltages are fully mitigated. This control concept can be summarized in the following statement: Overvoltage mitigation with minimum losses is achieved when a DG unit starts absorbing reactive power only when its PCC voltage is equal to the PCC voltage of the next
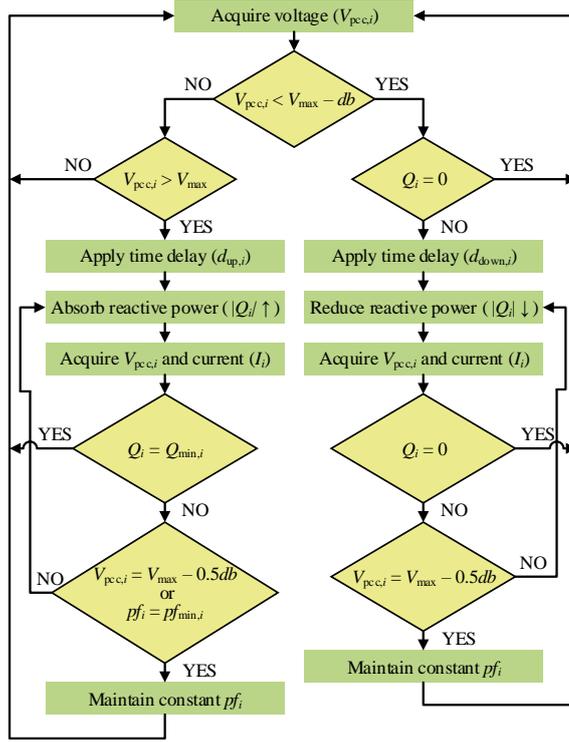
8

Figure 1: Reactive power control scheme of the DG unit connected to the i-th node.

downstream DG unit.

To implement this control concept, a coordinated control scheme is proposed. According to this, the DG unit connected to the i-th node is assigned to monitor and keep the PCC voltage ($V_{\text{pcc},i}$) at acceptable levels, following the procedure described in Fig. 1. This procedure describes the dynamic operation of each DG unit participating in the voltage regulation process and consists of two operation modes separated by a small deadband (db), where no actions occur in order to prevent oscillations and repeated activation-deactivation cycles.

The first operation mode corresponds to the overvoltage mitigation and is activated in case $V_{\text{pcc},i}$ exceeds V_{max}. Prior to the activation of this process, a time delay ($d_{\text{up},i}$) is introduced to attain a near-optimal reactive power allocation among the DG units, following the above-mentioned control concept. This time delay differs among the DG units and is determined by the central controller, considering the PCC voltage and the location of each DG unit. Afterwards, the DG unit starts absorbing reactive power by employing a proportional-integral (PI) controller to eliminate the error between $V_{\text{pcc},i}$ and the target voltage ($V_{\text{max}} - 0.5db$). This process continues up to the reactive power capability limit

9

of the DG unit unless either the voltage is successfully regulated or the network section power factor (NSPF) of the i-th node, i.e., the overall power factor (pf_i) seen from the i-th node and downstream, reaches the minimum one ($pf_{\min,i}$). In the latter two cases, the PI controller attempts to maintain a constant NSPF, resulting in a constant voltage drop at the i-th branch.

The constraint of minimum NSPF poses an upper limit to the reactive power flowing through the branch, which is calculated by

$$pf_{\min,i} = \cos(\arctan(-R_i/X_i)). \tag{14}$$

This value depends only on the line characteristics and derives from the *LinDistFlow* equations of [7], assuming a zero voltage drop between the associated nodes. The zero voltage drop indicates that there exist upstream nodes with voltages equal to or greater than that of the i-th node. Thus, this constraint is introduced to avoid the excessive and unnecessary reactive power consumption of this DG unit.

The second operation mode includes the reverse process of properly reducing the reactive power consumption. This is activated when $V_{\mathrm{pcc},i}$ falls below the voltage threshold ($V_{\max}-db$). After a predefined time delay ($d_{\mathrm{down},i}$), the DG unit reduces the reactive power till zero or till the voltage regulation is accomplished. In the latter case, the constant NSPF operation is activated.

It is evident that the DG units participating in the proposed control scheme should be overdimensioned to absorb reactive power, even at rated conditions. More specifically, a sufficient amount of reactive power must be always available to ensure the applicability of the above-mentioned control concept and thus the overvoltage mitigation with near-minimum active power losses. This amount is time-varying and can be approximately calculated by employing the *LinDistFlow* equations, assuming a zero voltage drop between two adjacent DG units:

$$Q_{\mathrm{av},i} = -\frac{\displaystyle\sum_{j\in N_{\mathrm{d},pd(i)}}\ \sum_{k\in B_{pd(i),j}\cap B_{pd(i),i}}(P_j R_k + Q_j X_k)}{\displaystyle\sum_{k\in B_{pd(i),i}} X_k} \tag{15}$$

where $Q_{\mathrm{av},i}$ is the required available reactive power of the DG unit located at the i-th

node, $pd(i)$ is the node of the previous adjacent DG unit, and $B_{pd(i),j}$ is the set of branches between the $pd(i)$ and the j-th node. It is worth mentioning that the oversizing factor can be estimated by employing (15) with generation and consumption forecasts. Nevertheless, this is considered beyond the scope of this paper.

3.2. Reactive power control of loads

In cases of smaller than required dimensioning of the DG units, their available reactive power may be inadequate for the effective voltage regulation. This usually occurs during high generation periods, where the DG units operate close to the rated active power and present a limited reactive power capability [13]. Therefore, the reactive power capability of DG units is potentially a limiting factor of the overall DG penetration. Additionally, there exists the possibility that the maximum network voltage will appear at nodes where only loads are connected.

To overcome these issues, the RPC of loads is proposed as a supplementary method to the overvoltage mitigation process. Generally, MV loads are equipped with reactive power compensation devices to improve their inherent lagging power factor. Thus, the occasional deactivation of these devices offers an additional reactive power sink, contributing to the regulation of network voltages. The RPC of loads is activated by the central controller when the following conditions are met: (1) overvoltages occur and (2) the DG units have reached their reactive power limits. To achieve near-minimum active power losses, according to the control concept of Section 3.1, this additional reactive power must be absorbed by the loads close to the nodes with overvoltages. Consequently, these loads in conjuction with the DG units are selected to contribute to the voltage regulation process. The reverse process of restoring the power factor of the loads is activated provided the reactive power of the DG units is zeroed and the voltages remain below the voltage threshold ($V_{\max} - db$).

3.3. OLTC operation

Within the framework of the proposed method, the OLTC operation fulfills two objectives. The primary objective is the regulation of network voltages within permissible limits. Since overvoltages can be fully tackled by the proposed RPC strategy based on the combined operation of DG units and loads, the OLTC control is employed for the mitigation of

11

undervoltages that may occur in passive feeders. Although the Standard EN 50160 poses a maximum voltage variation of $\pm 10\%$ of the nominal voltage [26], many DSOs adopt stricter limits in MV networks. In this paper, the permissible voltage variation is considered equal to $\pm 5\%$. The secondary objective is the reduction of network losses during high generation periods. This can be attained by decreasing the voltage magnitude of the MV busbar (V_{mv}) and thus of the network voltages to reduce the reactive power consumption of DG units and loads. The proposed OLTC operation can be expressed mathematically as follows:

$$
tap^{t+1} = \begin{cases} tap^t + 1, & \text{if } \mathbf{V}^{t+1} > V_{\min} \text{ and } \mathbf{V}^t \geq TV \\ tap^t - 1, & \text{if } V_{\mathrm{mv}}^{t+1} < 1.05 \text{ p.u. and} \\ & \qquad \mathbf{V}^t < V_{\min} \text{ or } \mathbf{V}^{t+1} < TV \\ tap^t, & \qquad \text{otherwise} \end{cases} \tag{16}
$$

where $\mathbf{V}^t$ denotes the vector of network voltages at time instant t and TV is the target voltage ($V_{\max} - 0.5db$). Assuming a tap change occurs, the network voltages at the next time instant ($\mathbf{V}^{t+1}$) can be estimated by adding a voltage variation ($\Delta \mathbf{V}$) to $\mathbf{V}^t$. This value refers to the voltage variation per tap change, plus a small value, indicating the small impact of the changing loading conditions. The OLTC uses a 4-minute time delay to prevent the activation-deactivation cycles.

3.4. Operation of the central controller

The principal objective of the central controller is twofold: To monitor the network and to ensure its near-optimal operation by means of minimising active power losses. This can be attained by coordinating the network elements, i.e. the DG units, the loads, and the OLTC, following the procedure described in the flowchart of Fig. 2. The operation of the central controller consists of four main steps, as presented in detail below:

Step 1: *Acquisition of network voltages.* At every time instant (t), the central controller receives the voltage magnitudes of the DG units and of the end nodes. This operation is activated at discrete time intervals ($\Delta \tau$), which are DSO-defined and may vary from seconds to minutes.

Step 2: *Coordination of the DG units operation.* Afterwards, the central controller coor-

12

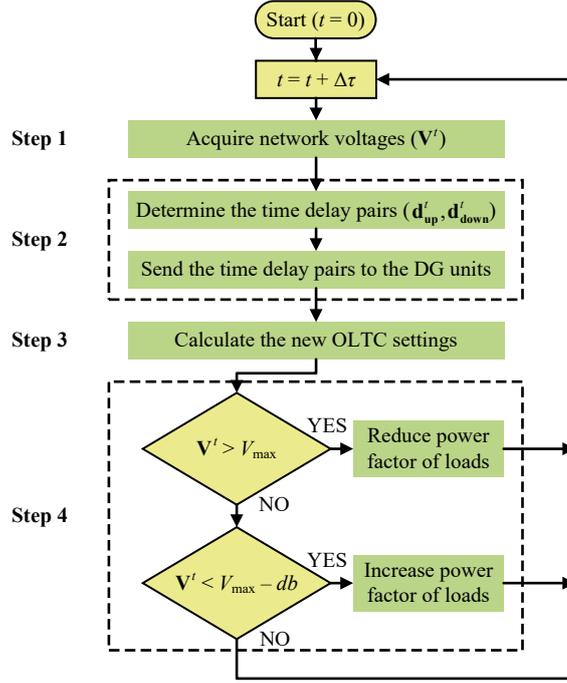Figure 2: Actions performed by the central controller at each time interval ($\Delta\tau$).

dinates the activation of the two operation modes in each DG unit by applying a set of time delays (d_{up}, d_{down}) to attain a near-optimal reactive power allocation that minimises network losses. In every time interval $\Delta\tau$, the time delays are updated and forwarded to each DG unit by the central controller, taking into account the corresponding PCC voltage and its location in the network.

Step 3: *OLTC operation.* Based on the acquired voltage measurements, (16) is employed to define the new tap position.

Step 4: *Participation of MV loads.* The time interval between two consecutive time instants is sufficient for the DG units to reach a new operational state. As a result, the existence of overvoltages at the next time instant indicates that the corresponding DG units have reached their reactive power capability limits. Thus, the central controller activates the RPC of the adjacent loads. The reverse process is implemented following a similar rationale, as shown in Fig. 2.

The time delay allocation is a low-complexity process, which prioritizes the response of DG units to implement the control concept of Section 3.1 and to ensure the effective voltage regulation of the network with near-minimum network losses. The time delays are determined by the central controller on a regular basis, i.e. at each time instant, exploiting the acquired
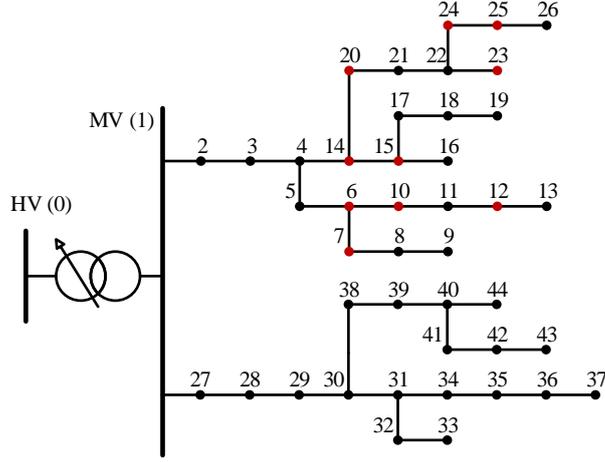
Figure 3: Topology of the examined network. The PV units are connected to the nodes with red color.

measurements and using the graph theory. More specifically, for a given time instant, the network voltages are structured in a tree, presenting the same topology with the electrical network. This tree is simplified by omitting nodes in order to form a strictly increasing voltage profile in each path between the root and a leaf node. The PCC voltages of the DG units connected to the omitted nodes are not critical for voltage regulation, since they are smaller than the corresponding of the adjacent DG units. Therefore, their participation in the voltage regulation process would increase network losses as shown in Section 3.1. To properly set the time delays at the remaining DG units of the simplified tree, the following conditions must be met:

1) The DG units of the same level nodes must present the same time delays in order to be activated simultaneously and to proportionally share the reactive power. According to the tree terminology, the node level is defined as the number of connections between the node and the root.

2) In each path, the time delays of the DG units are sorted based on the corresponding PCC voltages. Considering the first operation mode of overvoltage mitigation, high priority, i.e. small time delay, is given to the DG unit with the highest voltage. On the other hand, in the second operation mode, high priority is given to the DG unit with the lowest voltage.

3.5. Communication requirements

According to above-mentioned analysis, it is evident that a communication infrastructure is needed for the implementation of the proposed methodology. Due to the low data acquisi-

14

tion rate that strongly depends on the time interval $\Delta\tau$, low-bandwidth communication links can be employed to implement the proposed method. Alternatively, the proposed methodology can be integrated into the distribution management system (DMS) that already exists in several distribution networks including many functionalities, such as state estimation, fault location, service restoration, etc. [27].

To ensure the safe and reliable network operation within permissible voltage limits even in case of communication failure, the following actions must be taken by the basic network elements:

OLTC operation. The tap is automatically set to a low position to increase the network voltages and mitigate possible undervoltages.

DG units. Due to the absence of the time delay allocation process, the DG units will operate in an uncoordinated way, thus increasing the network losses. However, according to the proposed RPC strategy, overvoltages can be effectively addressed by the DG units.

MV Loads. The power factor of the loads which are located at or closed to nodes with overvoltages is set to the minimum value to contribute to the reactive power control of DG units.

4. Simulation results

The performance of the proposed coordinated voltage regulation strategy is evaluated on the 20 kV radial three-phase MV network of Fig. 3. The network characteristics concerning the length and the impedance of each line segment are presented in Tables 1 and 2, respectively. The line segments are numbered according to the downstream connection node. Although different DG technologies can be considered, only PV units are assumed in the simulated scenarios.

Moreover, the network consists of 10 photovoltaic (PV) units and 33 loads, numbered according to the connection node, with rated power, as shown in Table 3. The negative sign indicates active power consumption. The power factor of the loads with deactivated and activated compensation capacitor devices is 0.8 and 0.95 lagging, respectively. The nominal power factor of PV inverters is 0.85, which corresponds to an oversizing factor of 1.176. The voltage regulation deadband (*db*) is equal to 0.002 p.u. The 150 kV/20 kV transformer has

15

Table 1: Network lines length

Line segment number	Length (km)
3,8,18,26,29,30,34,42,43	1
2,6,7,10,11,13,17,21,24,27,32,36,39,40	2
4,9,12,15,19,20,23,25,28,33,35,37,38,41,44	3
5,14,16,22,31	4

Table 2: Network lines impedance

Line segment number	Impedance ($\mathbf{\Omega}$ /km)
2,3,4,27,28,29,30	$0.215+i0.334$
5,6,10,11,12,13,14,15,16,20,21,22, 24,25,26,31,32,33,38,39,40,41,42,43	$0.404+i0.386$
7,8,9,17,18,19,23,34,35,36,37,44	$0.576+i0.397$

rated power 50 MVA, short-circuit voltage 12%, whereas the full load losses are 0.5%. The OLTC range is ±8 with a voltage variation of 1.25% per tap.

In the next subsections, dynamic simulations are performed to validate the coordinated operation of PV units and loads. Furthermore, time-series simulations are employed to evaluate the long-term performance of the proposed method, compared to well-known decentralised and optimisation methods.

4.1. Dynamic simulations

Considering the examined network of Fig. 3, only the feeder comprising PV units is modelled at the PSIM software that is widely used for time-domain simulations. It is worth mentioning that in these simulations, a detailed modelling of all network elements is used to thoroughly evaluate the actual implementation of the proposed RPC method. In particular, the loads are modelled as constant power units, whereas the PV units are modelled using the full implementation of the grid-interfaced converters, including also the inherent control algorithms and the proposed RPC control algorithm as presented in the flowchart of Fig. 1. The voltage of the MV busbar is kept constant to 1.05 p.u. The PV units and the loads operate at their rated power for the whole simulation period, expect those depicted in Fig. 5b. The reactive power of the PV units participating in the voltage regulation process and the corresponding voltages are presented in Figs. 5a and 5c, respectively. The RPC of PV units is activated at 0.1 s.

Table 3: Rated active power of PV units and loads

Nodes	MW	Nodes	MW	Nodes	MW
7	0.60	6,14	2.00	10,20,25	1.00
12	0.70	8,37	-0.20	4,22,27,38,40	-0.60
13	-0.90	15,24	1.50	5,17,26,30,41	-0.30
23	0.50	29,35	-0.80	9,19,28,42,44	-0.40
31	-1.00	32,33	-0.70	2,11,21,34,36,43	-0.50
39	-1.20	3,16,18	-0.25		

Figure 4: Time delay allocation. a) Network topology with voltages and b) the corresponding tree with the calculated time delays.

Prior to the activation of the RPC, the allocation of the time delays among the PV units is carried out following the procedure described in Section 3.4. In particular, the tree of Fig. 4a, comprising the initial network voltages, is simplified to the tree of Fig. 4b to form a strictly increasing voltage profile in each path between the root and a leaf node. Considering the first operation mode of overvoltage mitigation, the highest priority, i.e. instant reaction on voltage changes, is given to PV25, whereas the lowest is given to PV14 and PV6. PV23 and PV24 belong to the same level nodes and thus the same time delay is applied to simultaneously activate the RPC and achieve a proportional reactive power sharing. The time delays between sequential level nodes, depend on the response of the PV units, which is very small for typical grid-interfaced inverters. In these simulations, it is considered equal to 0.2 s.

According to Fig. 4, PV25 reacts instantly against overvoltage limit violation by absorbing reactive power till the reactive power capability limit is reached at 0.13 s. The next PV units in the RPC activation sequence are PV23 and PV24 that are simultaneously activated after a time delay of 0.2 s. In this way, a proportional reactive power sharing is achieved among the PV units, while the corresponding voltages are reduced, as shown in Figs. 5a and 5c, respectively. At 0.5 s, PV20 starts absorbing reactive power up to its capability limit
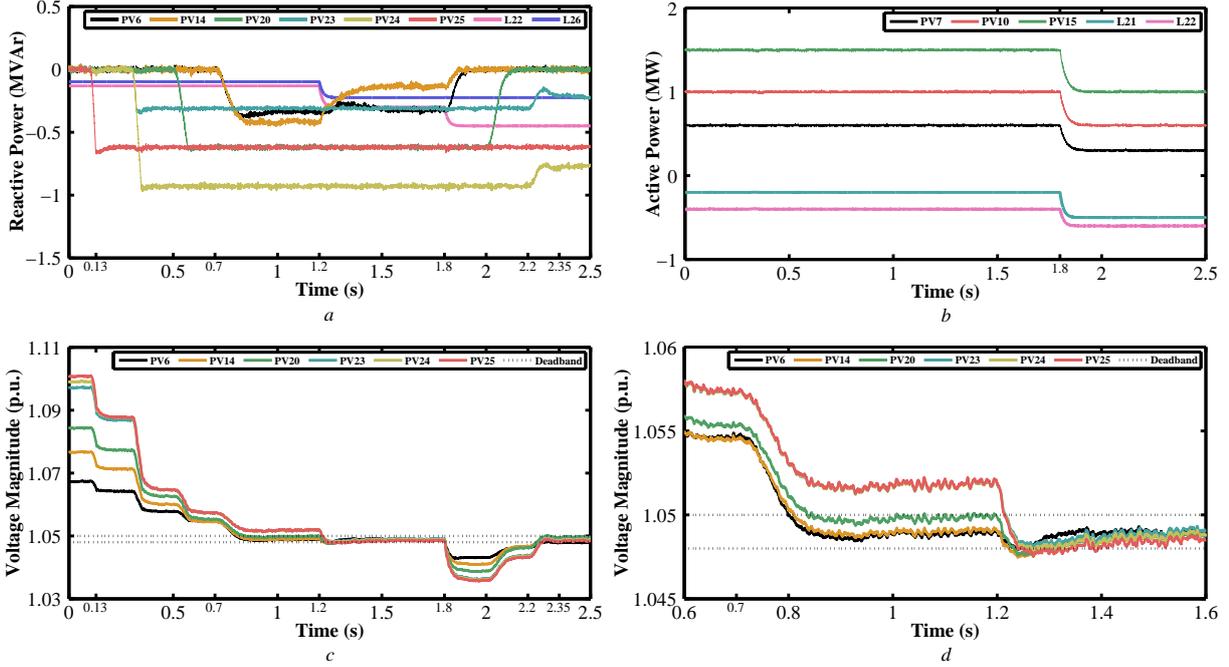
17

Figure 5: Time-domain simulations. a) Reactive power of PV units where negative values denote under-excitation, b) active power variation of PV units and loads, c) voltage profile magnitudes and d) voltage profile magnitudes (zoomed around overvoltage mitigation instant).

and finally, the RPC of PV6 and PV14 is simultaneously activated at 0.7 s to regulate the corresponding PCC voltages. At 1 s, the PCC voltages of PV6 and PV14 are regulated and the PV units switch to constant NSPF operation. According to Fig. 5c, the overvoltages have been successfully mitigated for all PV units expect PV23, PV24, and PV25. This happens due to the limited reactive power capability of these PV units. To overcome this burden, the RPC of the adjacent loads, i.e. L22 and L26, is initiated at 1.2 s by deactivating the reactive power compensation devices, thus reducing the corresponding power factor from 0.95 to 0.8 lagging. This surplus of reactive power reduces the voltages within permissible limits, as verified in Fig. 5c. Furthermore, the reactive power of PV14 is reduced, since it operates in constant NSPF mode.

To activate the reverse process of the coordinated reduction of the reactive power, the network voltages are reduced below the lower threshold $(V_{\max} - db)$ at 1.8 s. This is achieved by varying the active power of the PV units and loads of Fig. 5b, without, however, affecting the tree of Fig. 4b and the already implemented time delay allocation. More specifically, in all PV units, a voltage reduction below the lower threshold $(V_{\max} - db)$ occurs but, according to Fig. 4b, only PV6 and PV14 instantly react by reducing their reactive power till zero. After a time delay of 0.2 s, PV20 zeroes its reactive power consumption and finally at 2.2 s,

18

Table 4: Settings of the $Q(V)$ droop control scheme

PV unit	PV6	PV7	PV10	PV12	PV14
V_{th}^{QV} (p.u.)	1.0326	1.0320	1.0269	1.0384	1.0392
V_{max}^{QV} (p.u.)	1.0500	1.0500	1.0500	1.0500	1.0500
PV unit	PV15	PV20	PV23	PV24	PV25
V_{th}^{QV} (p.u.)	1.0384	1.0408	1.0442	1.0446	1.0450
V_{max}^{QV} (p.u.)	1.0500	1.0500	1.0500	1.0500	1.0500

PV23 and PV24 are activated simultaneously and reduce their reactive power till the voltage is finally regulated at 2.35 s. Afterwards, PV23 and PV24 operate at constant NSPF mode. In this way, an near-optimal reactive power allocation among the PV units is achieved.

4.2. Long-term evaluation

In this section, time-series simulations are performed to compare the proposed voltage regulation strategy with a decentralised and a centralised optimisation-based method. In the decentralised control scheme, the PV units are equipped with $Q(V)$ droop characteristics and the OLTC operates in automatic voltage regulation (AVR) mode. The settings of the $Q(V)$ droop curves, which are calculated following the coordination procedure of [12], are presented in Table 4. Concerning the AVR characteristics, the target voltage at the MV busbar is 1.05 p.u. with a deadband of 0.014 p.u. and 4 minutes time delay. Considering the optimisation-based method, (1)-(11) are solved in each time instant using the interior point technique implemented in MATLAB. Furthermore, the time-series simulations of the proposed and the decentralised control schemes are conducted using the simulation tool developed in [28].

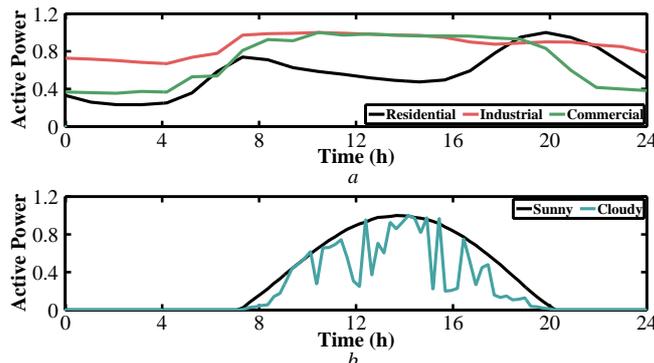The simulation period is one day with 1 minute time interval. Normalised generation and

Figure 6: Normalised profiles. a) Consumption profiles and b) generation profiles.

19

Table 5: Daily energy losses (MWh)

	Decentralised	Proposed	Optimised
	10.309	9.596	9.580
Difference (%)	+7.61	+0.17	0.00

consumption profiles, similar to those of Fig. 6, are arbitrary distributed to the PV units and loads, respectively. The overall reactive power consumption of the PV units is depicted in Fig. 7a, while the voltages of two indicative network nodes are shown in Figs. 7b and 7d, respectively. Additionally, the tap changes of the HV/MV transformer OLTC are presented in Fig. 7c, while the power losses and the daily energy losses of the network are presented in Fig. 8 and Table 5.

The decentralised method results in an increased reactive power consumption and thus increased energy losses, due to two main reasons. The first is related with the reactive power consumption of the PV units which is activated in lower voltages than the maximum permissible limit due to the existence of the droop characteristic. The second reason is the AVR operation, which maintains a constant voltage at the MV busbar close to 1.05 p.u. even during high generation periods, leading the PV units to absorb more reactive power. This can be also observed in Fig. 7c where the tap position of the decentralised method follows a different pattern compared to the proposed and optimisation-based methods.

The proposed control strategy regulates effectively the network voltages as shown in Figs. 7b and 7d, while, according to Fig. 7a, the reactive power consumption is reduced compared to the decentralised method. As a result, the energy losses are reduced, as presented in Table 5. In comparison with the optimisation method, the proposed method presents a similar performance, indicating that the proposed method can ensure near-optimal solutions with reduced computational complexity. Furthermore, in case of communication loss or failure of the central controller, overvoltages may occur in the optimisation-based method, since the network operation is strongly dependent on the central controller. On the other hand, in the proposed method, the PV units operate autonomously, but in a coordinated way, thus ensuring the overvoltage mitigation regardless the state of the central controller.
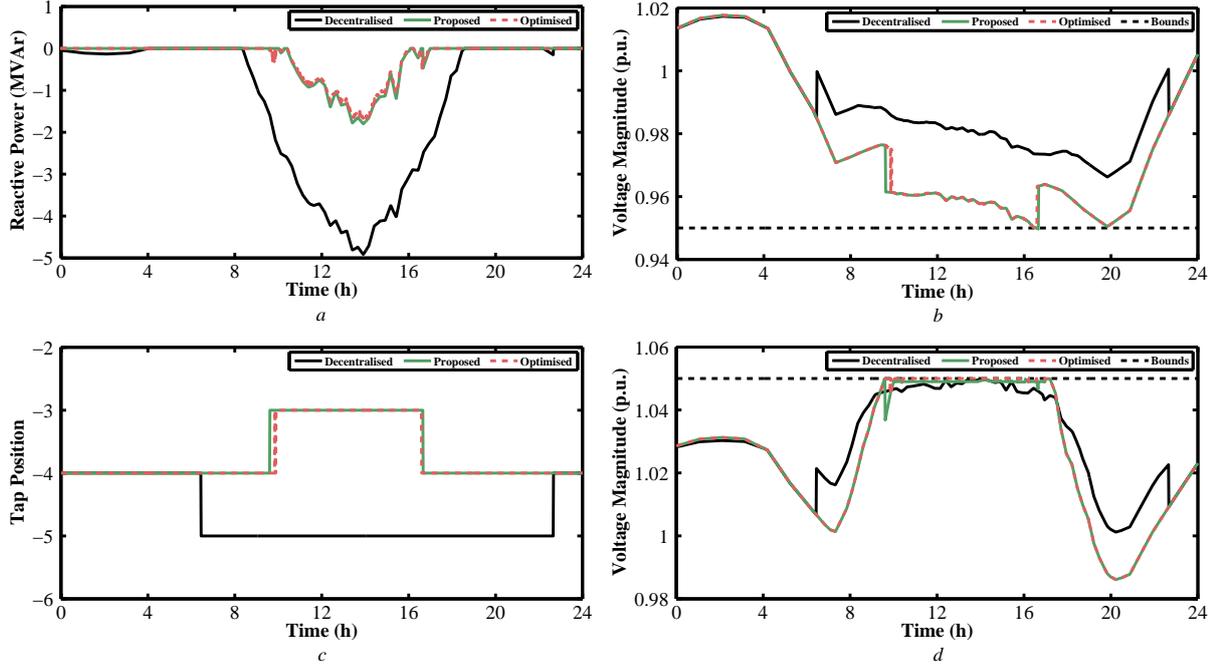
Figure 7: Time-series simulations. a) Reactive power of PV units, b) voltage profiles of node 37, c) tap variation profile, and d) voltage profiles of node 25.
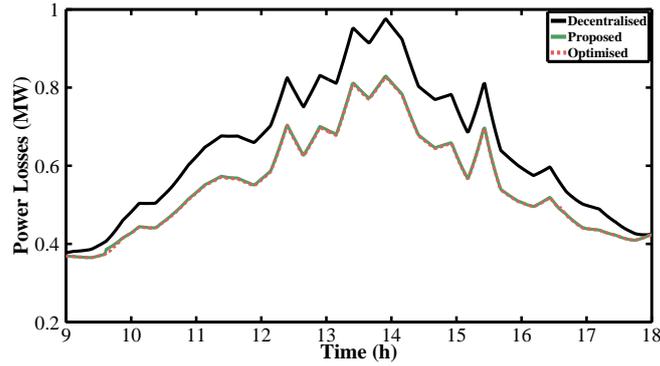

Figure 8: Total network power losses between 9:00 and 18:00.

5. Conclusions

In this paper, the problem of optimal voltage regulation is addressed by developing a generalised and straightforward control strategy. The proposed technique implements a distinct time delay allocation feature, based on the graph theory, which ensures the near-optimal reactive power allocation among the DG units. The proposed method is further enhanced with the active participation of specific MV loads in the voltage regulation process, contributing in the reactive power consumption.

The validity of the proposed method is tested on a radial MV network by performing time-domain and time-series simulations. The proposed coordinated voltage regulation strategy presents a superior performance compared to the decentralised methods, regarding energy

losses and the overall reactive power consumption. On the other hand, it presents a similar performance to the optimisation-based method, with reduced computational complexity and communication needs. Therefore, it can be readily used to efficiently tackle overvoltages in the MV distribution networks.

References

[1] M. Madrigal, M. Bhatia, G. Elizondo, A. Sarkar, M. Kojima, Twin peaks: Surmounting the global challenges of energy for all and greener, more efficient electricity services, IEEE Power Energy Mag. 10 (3) (2012) 20–29. `doi:10.1109/MPE.2012.2188666`.

[2] F. Careri, C. Genesi, P. Marannino, M. Montagna, S. Rossi, I. Siviero, Generation expansion planning in the age of green economy, IEEE Trans. Power Syst. 26 (4) (2011) 2214–2223. `doi:10.1109/TPWRS.2011.2107753`.

[3] C. L. Masters, Voltage rise: the big issue when connecting embedded generation to long 11 kv overhead lines, Power Eng. J. 16 (1) (2002) 5–12. `doi:10.1049/pe:20020101`.

[4] V. Calderaro, G. Conio, V. Galdi, A. Piccolo, Reactive power control for improving voltage profiles: A comparison between two decentralized approaches, Elect. Power Syst. Res. 83 (1) (2012) 247–254. `doi:10.1016/j.epsr.2011.10.010`.

[5] G. Mokhtari, G. Nourbakhsh, A. Ghosh, Smart coordination of energy storage units (ESUs) for voltage and loading management in distribution networks, IEEE Trans. Power Syst. 28 (4) (2013) 4812–4820. `doi:10.1109/TPWRS.2013.2272092`.

22

[6] P. M. S. Carvalho, P. F. Correia, L. A. F. M. Ferreira, Distributed reactive power generation control for voltage rise mitigation in distribution networks, IEEE Trans. Power Syst. 23 (2) (2008) 766–772. `doi:10.1109/TPWRS.2008.919203`.

[7] K. Turitsyn, P. Sulc, S. Backhaus, M. Chertkov, Local control of reactive power by distributed photovoltaic generators, in: Proc. First IEEE Int. Conf. Smart Grid Communications, 2010, pp. 79–84. `doi:10.1109/SMARTGRID.2010.5622021`.

[8] G. C. Kryonidis, C. S. Demoulias, G. K. Papagiannis, A nearly decentralized voltage regulation algorithm for loss minimization in radial MV networks with high DG penetration, IEEE Trans. Sustain. Energy 7 (4) (2016) 1430–1439. `doi:10.1109/TSTE.2016.2556009`.

[9] A. R. D. Fazio, G. Fusco, M. Russo, Decentralized control of distributed generation for voltage profile optimization in smart feeders, IEEE Trans. Smart Grid 4 (3) (2013) 1586–1596. `doi:10.1109/TSG.2013.2253810`.

[10] E. Demirok, P. C. Gonzàlez, K. H. B. Frederiksen, D. Sera, P. Rodriguez, R. Teodorescu, Local reactive power control methods for overvoltage prevention of distributed solar inverters in low-voltage grids, IEEE J. Photovolt. 1 (2) (2011) 174–182. `doi:10.1109/JPHOTOV.2011.2174821`.

[11] A. Samadi, R. Eriksson, L. Söder, B. G. Rawn, J. C. Boemer, Coordinated active power-dependent voltage regulation in distribution grids with PV systems, IEEE Trans. Power Del. 29 (3) (2014) 1454–1464. `doi:10.1109/TPWRD.2014.2298614`.

[12] A. Samadi, E. Shayesteh, R. Eriksson, B. Rawn, L. Söder, Multi-objective coordinated droop-based voltage regulation in distribution grids with PV systems, Renew. Energy 71 (2014) 315–323. `doi:10.1016/j.renene.2014.05.046`.

[13] V. Calderaro, G. Conio, V. Galdi, G. Massa, A. Piccolo, Optimal decentralized voltage control for distribution systems with inverter-based distributed generators, IEEE Trans. Power Syst. 29 (1) (2014) 230–241. `doi:10.1109/TPWRS.2013.2280276`.

[14] S. Bolognani, R. Carli, G. Cavraro, S. Zampieri, Distributed reactive power feedback control for voltage regulation and loss minimization, IEEE Trans. Autom. Control 60 (4) (2015) 966–981. `doi:10.1109/TAC.2014.2363931`.

[15] B. A. Robbins, C. N. Hadjicostis, A. D. Domínguez-García, A two-stage distributed architecture for voltage control in power distribution systems, IEEE Trans. Power Syst. 28 (2) (2013) 1470–1482. `doi:10.1109/TPWRS.2012.2211385`.

[16] M. A. Azzouz, M. F. Shaaban, E. F. El-Saadany, Real-time optimal voltage regulation for distribution networks incorporating high penetration of PEVs, IEEE Trans. Power Syst. 30 (6) (2015) 3234–3245. `doi:10.1109/TPWRS.2014.2385834`.

[17] M. E. Baran, I. M. El-Markabi, A multiagent-based dispatching scheme for distributed generators for voltage support on distribution feeders, IEEE Trans. Power Syst. 22 (1) (2007) 52–59. `doi:10.1109/TPWRS.2006.889140`.

[18] M. Brenna, E. D. Berardinis, L. D. Carpini, F. Foiadelli, P. Paulon, P. Petroni, G. Sapienza, G. Scrosati, D. Zaninelli, Automatic distributed voltage control algorithm in smart grids applications, IEEE Trans. Smart Grid 4 (2) (2013) 877–885. `doi:10.1109/TSG.2012.2206412`.

[19] A. Kulmala, S. Repo, P. Järventausta, Coordinated voltage control in distribution networks including several distributed energy resources, IEEE Trans. Smart Grid 5 (4) (2014) 2010–2020. `doi:10.1109/TSG.2014.2297971`.

[20] Y. P. Agalgaonkar, B. C. Pal, R. A. Jabr, Distribution voltage control considering the impact of PV generation on tap changers and autonomous regulators, IEEE Trans. Power Syst. 29 (1) (2014) 182–192. `doi:10.1109/TPWRS.2013.2279721`.

[21] F. A. Viawan, D. Karlsson, Voltage and reactive power control in systems with synchronous machine-based distributed generation, IEEE Trans. Power Del. 23 (2) (2008) 1079–1087. `doi:10.1109/TPWRD.2007.915870`.

[22] V. Calderaro, V. Galdi, F. Lamberti, A. Piccolo, A smart strategy for voltage control

ancillary service in distribution networks, IEEE Trans. Power Syst. 30 (1) (2015) 494–502. `doi:10.1109/TPWRS.2014.2326957`.

[23] H. G. Yeh, D. F. Gayme, S. H. Low, Adaptive VAR control for distribution circuits with photovoltaic generators, IEEE Trans. Power Syst. 27 (3) (2012) 1656–1663. `doi: 10.1109/TPWRS.2012.2183151`.

[24] S. Weckx, C. Gonzalez, J. Driesen, Combined central and local active and reactive power control of PV inverters, IEEE Trans. Sustain. Energy 5 (3) (2014) 776–784. `doi:10.1109/TSTE.2014.2300934`.

[25] M. E. Elkhatib, R. El-Shatshat, M. M. A. Salama, Novel coordinated voltage control for smart distribution networks with DG, IEEE Trans. Smart Grid 2 (4) (2011) 598–605. `doi:10.1109/TSG.2011.2162083`.

[26] Voltage Characteristics of Electricity Supplied by Public Distribution Networks (2010).

[27] H. Ahmadi, J. R. Martí, H. W. Dommel, A framework for Volt-VAR optimization in distribution systems, IEEE Trans. Smart Grid 6 (3) (2015) 1473–1483. `doi:10.1109/ TSG.2014.2374613`.

[28] G. C. Kryonidis, E. O. Kontis, A. I. Chrysochos, C. S. Demoulias, D. Bozalakov, B. Meersman, T. L. Vandoorn, L. Vandevelde, A simulation tool for extended distribution grids with controlled distributed generation, in: PowerTech, 2015 IEEE Eindhoven, 2015, pp. 1–6. `doi:10.1109/PTC.2015.7232778`.